PROTEINS: Structure, Function, and Genetics 47:86–96 (2002)
DOI 10.1002/prot.10058

Noncovalent Interaction Energies in Covalent Complexes: TEM-1 β-Lactamase and β-Lactams

Xiaojun Wang, George Minasov, and Brian K. Shoichet*
Department of Molecular Pharmacology and Biological Chemistry, Northwestern University, Chicago, Illinois

ABSTRACT **The class A β-lactamase TEM-1 is a key bacterial resistance enzyme against β-lactam antibiotics, but little is known about the energetic bases for complementarity between TEM-1 and its inhibitors. Most inhibitors form a covalent adduct with the catalytic Ser70, making the measurement of equilibrium constants, and hence interaction energies, technically difficult. This study evaluates noncovalent interactions within covalent complexes by examining the differential stability of TEM-1 and its inhibitor adducts. The thermal denaturation of TEM-1 follows a two-state, reversible model with a melting temperature (T_m) of 51.6°C and a van't Hoff enthalpy of unfolding (ΔH_{VH}) of 146.2 kcal/mol at pH 7.0. The stability of the enzyme changes on forming an inhibitor adduct. As expected, some inhibitors stabilize TEM-1; transition-state analogues increase the T_m by up to 3.7°C (1.7 kcal/mol). Surprisingly, all β-lactam covalent acyl–enzyme complexes tested destabilize TEM-1 significantly relative to the apo-enzyme. For instance, the clinically used inhibitor clavulanic acid and the β-lactamase-resistant β-lactams moxalactam and imipenem destabilize TEM-1 by over 2.6°C (1.2 kcal/mol) in their covalent adducts. Based on the structure of the TEM-1/imipenem complex (Maveyraud et al., J Am Chem Soc 1998;120:9748–52), destabilization by moxalactam and imipenem is thought to be caused by a steric clash between the side-chain of Asn132 and the 6(7)-α group of these β-lactams. To test this hypothesis, the mutant enzyme N132A was made. In contrast with wild-type, the covalent complexes between N132A and both imipenem and moxalactam stabilize the enzyme, consistent with the hypothesis. To investigate the structural bases of this dramatic change in stability, the structure of N132A/imipenem was determined by X-ray crystallography. In the complex with N132A, imipenem adopts a very different conformation from that observed in the wild-type complex, and the putative destabilizing interaction with residue 132 is relieved. Studies of several enzymes suggest that β-lactams, and covalent inhibitors in general, can have either net favorable or net unfavorable noncovalent interaction energies within the covalent complex. In the case of TEM-1, such unfavorable interactions convert substrate analogues into very effective inhibitors. Proteins 2002;47:86–96.** © 2002 Wiley-Liss, Inc.

Key words: protein stability; TEM-1; β-lactamase; β-lactam; antibiotic resistance

INTRODUCTION

TEM-1 β-lactamase hydrolyzes β-lactams such as the penicillins and the cephalosporins. This process is the most widespread mechanism of bacterial resistance to β-lactam antibiotics and poses a growing threat to public health.[1] Despite intense study, it has been difficult to determine the interaction energies between β-lactams and TEM-1 or between any class A β-lactamase and β-lactams (but see Matagne and coworkers for recent progress[2]).

β-Lactams rapidly form a covalent acyl intermediate through nucleophilic attack by Ser70 of TEM-1 on the strained lactam ring (Fig. 1). The deacylation step determines the fate of β-lactams. When deacylation is fast, the β-lactam is a substrate; when deacylation is slow, the β-lactam acts as an inhibitor, forming a long-lived acyl adduct. The formation of such a covalent adduct is essentially irreversible, as there is no measurable reverse reaction to the closed β-lactam ring. Interaction energies, which depend on reversible equilibria, are thus not readily obtained from K_m or IC_{50} values from conventional steady-state kinetics. This limits our ability to interpret structure for the function of this enzyme. Although several elegant structural studies of β-lactam interactions with TEM-1 and related class A β-lactamases[3–7] have been carried out, understanding the interactions observed quantitatively in the structures has been difficult because all reflect an irreversible reaction.

An alternative to measuring equilibrium binding constants is to determine the effects of covalent adduct formation on the reversible stability of an enzyme. The differential stability between an apo-enzyme and a ligand–

Abbreviations: ΔC_p, change in heat capacity at constant pressure; ΔH_{VH}, van't Hoff enthalpy of unfolding; ΔS_u, entropy of unfolding; ΔG_u, Gibbs free energy of unfolding; CD, circular dichroism; PBP, penicillin-binding protein; T_m, melting temperature; UV, ultraviolet; ESBL, extended spectrum β-lactamase; IRT, inhibitor-resistant TEM-type β-lactamase; WT, wild-type.

Grant sponsor: National Science Foundation; Grant number: MCB97344484; Grant sponsor: DuPont Co.; Grant sponsor: Dow Chemical Co.; Grant sponsor: State of Illinois; Grant sponsor: U.S. Department of Energy; Contract number: W-31-102-Eng-38.

*Correspondence to: Brian K. Shoichet, Department of Molecular Pharmacology and Biological Chemistry, Northwestern University, 303 E. Chicago Avenue, Chicago, IL 60611-3008. E-mail: b-shoichet@northwestern.edu.

Received 29 March 2001; Accepted 19 October 2001

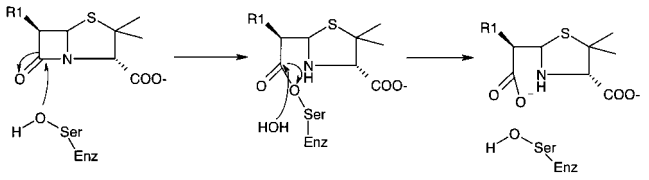

Fig. 1. Simplified schematic mechanism of TEM-1 β-lactamase. The acyl adduct intermediate is long-lived for the β-lactams studied.

enzyme complex reflects the noncovalent interaction energies between the ligand and the enzyme.[8–10] If denaturation is two-state and reversible, the noncovalent interaction can be determined through a thermodynamic cycle (Fig. 2). One assumption implicit in this cycle is that there is little noncovalent interaction between the β-lactams and the enzyme in the denatured state; i.e., there is little change in the stability of the denatured state of the apo- versus the ligand-bound enzyme ($\Delta G_2 \approx 0$, Fig. 2). A second assumption is that the covalent interaction energy between the ligand and the enzyme remains unchanged going from the folded to the unfolded state. These assumptions are widely used in the analysis of stability changes in site-directed mutant proteins; nevertheless, the quantitative conclusions reached in this study are reliable only to the extent that they are correct. The method of differential stability is well suited to enzymes, such as TEM-1, that form long-lived covalent adducts, as these will be stable throughout the denaturation transition and will not be subject to secondary equilibria.[8,10] The method thus provides an alternative to traditional binding or kinetic equilibria in just those cases in which such equilibria are least available.

Differential stability was used by Pratt and colleagues to investigate interactions between PC1 β-lactamase and transition-state analogues to determine how well these irreversible inhibitors captured the stabilization afforded by the enzyme to the high-energy intermediate.[8] Previously, we used differential stability to measure interaction energies between β-lactams and the penicillin-binding protein, PBP5, from *Escherichia coli*[11] and between β-lactams and the class C β-lactamase AmpC.[10] In the case of PBP5, all β-lactams that formed long-lasting adducts stabilized the enzyme, indicating that they complemented the binding site. In the case of AmpC β-lactamase, some inhibitors stabilized the enzyme, but others actually destabilized it, indicating that some formed unfavorable noncovalent interactions in the covalent adducts. Although a covalent inhibitor does not have to have favorable noncovalent interactions, one typically assumes that they will. In an attempt to investigate how general this result might be, we have turned to the class A β-lactamase TEM-1, which is widely studied both as a model enzyme and as an antibiotic resistance target.[12] Although there is an evolutionary relationship among PBP5, AmpC, and TEM-1,[13,14] it is a distant relationship, and the enzymes have different substrate and inhibition profiles. To our surprise, we found that none of the β-lactams we investigated had favorable noncovalent interaction energies with TEM-1; i.e., they did not fit the site well within the acyl adduct. Instead, all the β-lactams studied destabilized the enzyme in the acyl adduct. The interactions between TEM-1 and many of these β-lactam inhibitors therefore occupy one end of a spectrum of possibilities for complementarity in covalent adducts.

For two of the inhibitors studied, imipenem and moxalactam, the poor complementarity within the covalent adduct appears to be attributable to an unfavorable contact between a ligand group and the side-chain of Asn132. This is based on the X-ray crystal structure of the TEM-1/imipenem complex[7] and, by analogy, the X-ray crystal structure of moxalactam in complex with the β-lactamase AmpC.[15] To investigate the extent to which this single close contact contributes to the observed destabilization, the substitution Asn132 → Ala was made. In contrast with the wild-type enzyme, this mutant was actually stabilized by imipenem and moxalactam. To investigate the structural bases of this dramatic change in stability, the structure of the complex between imipenem and N132A was determined by X-ray crystallography to 1.73 Å resolution. A comparison of the mutant and WT complexes suggests that these clinically used β-lactams have a mechanism of enzyme destabilization.[3,7,15,16]

MATERIALS AND METHODS

Enzyme Preparation

The TEM-1 wild-type gene was amplified from pBR322 by polymerase chain reaction (PCR). An artificial promoter sequence from pRZ3 (kindly provided by Dr. R.G. Kemp) was linked to the 5′ end of the TEM-1 gene, again by PCR. The linked product was digested with *Hin*dIII and *Bam*HI and ligated into the *Hin*dIII and *Bam*HI-treated pAlter Ex II (Promega, Madison, WI). The pAlter Ex II TEM-1 plasmid was used to transform *Escherichia coli* JM109 cells. TEM-1 was expressed and purified in a procedure modified from Dubus et al.[17] The protein was produced at room temperature in 2 × YT medium. Cells were collected by centrifugation and resuspended in 5 mM Tris-HCl, at pH 8.0, containing 1 mM EDTA and 20% (w/v) sucrose at room temperature for 10 min. Cells were then collected and resuspended in ice-cold 5 mM $MgCl_2$ for 10 min. The supernatant was saved as the periplasmic contents, concentrated to ~100 ml, and dialyzed against 5 mM Tris-HCl, at pH 8.0. The crude extract was applied to a Q-Sepharose Fast Flow column (Pharmacia, Uppsala, Sweden) equilibrated with 5 mM Tris-HCl, pH 8.0. The column was then washed extensively with 5 mM Tris-HCl, at pH 8.0. The enzyme was eluted by 5 mM Tris-HCl, at pH 8.0, containing 100 mM NaCl. The active fractions were pooled and dialyzed against 100 mM sodium phosphate, at pH 8.0. The protein was then applied to a Ni^{2+}-nitrilotriacetate–agarose column (Qiagen, Valencia, CA) equilibrated in the same buffer. The enzyme was eluted by 40 mM imidazole. The enzyme solution was concentrated to 6 mg/ml and stored in 200 mM potassium phosphate, at pH 7.0, 50% glycerol at −20°C.

Preparation of TEM-1 Mutant N132A

Site-directed mutagenesis was carried out using a modified two-step PCR protocol.[18] In the first step, two PCRs

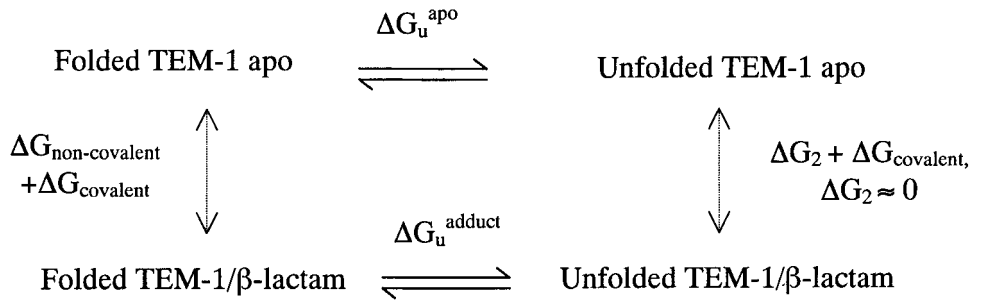

$$\Delta G_{\text{non-covalent}} + \Delta G_{\text{covalent}} + \Delta G_u^{\text{adduct}} - \Delta G_u^{\text{apo}} - \Delta G_2 - \Delta G_{\text{covalent}} = 0$$
$$\therefore \Delta G_{\text{non-covalent}} = \Delta G_u^{\text{apo}} + \Delta G_2 - \Delta G_u^{\text{adduct}}$$
$$= \Delta G_u^{\text{apo}} - \Delta G_u^{\text{adduct}}$$
$$= \Delta\Delta G_u$$

Fig. 2. Thermodynamic cycle for determining noncovalent interaction energies within covalent complexes by differential stability. The acyl adduct form of the TEM-1/β-lactam complex is represented.

were performed: one reaction involved a mutagenesis antisense primer and a sense primer that covered the *Nde*I site flanking the 5′ end of the gene, and the second reaction involved a sense mutagenesis primer and an antisense primer covering the *Eco*RI site flanking the 3′ end of the gene. The reaction in 100 μl included 2.5 U of *Pfu* DNA polymerase (Stratagene), reaction buffer (Stratagene), 100 ng of pAlter Ex II TEM-1, 250 ng of flanking primer, 250 ng of mutagenesis primer, and each dNTP at 0.2 mM. The PCR products were purified with QIAquick Gel Extraction kit (Qiagen). In the second step, PCR was performed in the same buffer using 100 ng of each of the first-round products and 250 ng of each flanking primer. The PCR product was purified with the QIAquick PCR Purification kit (Qiagen) and digested with *Nde*I and *Eco*RI. The digested product was again purified with the QIAquick PCR Purification kit, subsequently ligated into pAlter Ex II TEM-1 plasmid predigested with *Nde*I and *Eco*RI, and then transformed into JM109 cells. The modified pAlter Ex II TEM-1 was subsequently purified and sequenced, to verify the mutation. The N132A mutant plasmid was then transformed into JM109 cells. N132A was expressed and purified as described for the wild-type enzyme.

Thermal Denaturation

Thermal denaturation was carried out in 200 mM potassium phosphate at pH 7.0. The buffer was prepared by mixing dibasic potassium phosphate (ACS reagent grade from Sigma, St. Louis, MO) and monobasic potassium phosphate (ACS reagent grade from Aldrich Chemical, Milwaukee, WI) and adjusted by phosphoric acid or potassium hydroxide to pH 7.0. Moxalactam was purchased from Sigma.

Inhibitor adducts were formed by mixing an enzyme solution in buffer with 70–100-fold molar excess of an inhibitor, at room temperature, except for imipenem, for which a saturated imipenem solution was mixed with equal volume of enzyme solution (200-fold molar excess of imipenem). This procedure adopts that used to produce an imipenem/TEM-1 WT complex whose structure was determined by X-ray crystallography.[7] Incubation times were 5 min to a half-hour, unless otherwise noted. An aliquot of this solution was added to 3.5 ml of pre-equilibrated buffer solution. The enzyme or enzyme adduct was denatured by raising the temperature in 0.1°C increments at a ramp rate of 2°C/min, unless otherwise noted. Denaturation was marked by an obvious transition in both the far-ultraviolet (UV) circular dichroism (CD) and fluorescence signals (below). To produce the largest reproducible T_m change, long incubation times were required for compound 1, which acylates the enzyme slowly.

Values of $\Delta\Delta G_u$ were determined by Schellman's method for all enzymes and enzyme–inhibitor complexes[19]:

$$\Delta\Delta G_u = \Delta T_m \cdot \Delta S_{\text{apo-enzyme}} \quad (1)$$

Values of $\Delta\Delta G_u$ were also determined by comparing the equilibria of unfolding directly using the Gibbs–Helmholtz equation (eq. 2). The reference temperature (T^0) was set to a temperature in the middle of the range of the unfolding T_m values; conveniently, this was T_m of the apo-enzyme (51.6°C for TEM-1 and 49.6°C for N132A). At this reference temperature, the ΔG_u for the apo-enzyme was zero:

$$\Delta\Delta G_u = \Delta G_u - \Delta G_u^{\text{apo}}$$
$$= \Delta H^0 - T\Delta S^0 + \Delta C_p[T - T^0 - T\ln(T/T^0)] \quad (2)$$

An increase in T_m indicates stabilization of the adduct relative to the apo-enzyme and a positive $\Delta\Delta G_u$ value. A decrease in T_m indicates destabilization of the adduct relative to the apo-enzyme and a negative $\Delta\Delta G_u$ value.

CD Measurement

CD measurements were performed on a Jasco J-715 spectropolarimeter with a Jasco PTC-348WI Peltier-effect

temperature controller. Superasil quartz cells with a 1-cm path length from Hellma (Jamaica, NY) were used for all experiments. For melting, an in-cell temperature probe and stir bar were used. All T_m and ΔH_{VH} values were calculated with the EXAM program[20]; the change in heat capacity upon denaturation (ΔC_p) was set to 3.8 kcal/mol · K (16.0 kJ/mol · K) for each enzyme and complex.

The helical content of samples was monitored by CD in the far-UV region at 223 or 232 nm, with the higher wavelength used to reduce light absorption by inhibitors. The behavior of the apo-protein was identical at both wavelengths. Tertiary structure was monitored by CD in the near-UV region at 270 nm.

Fluorescence Measurements

Fluorescence experiments were carried out in the Jasco J-715 spectropolarimeter with a fluorescence attachment, which allowed us to monitor melting by CD and fluorescence simultaneously. The emission fluorescence was monitored using a cut-on a 300-nm filter, reflecting the 340-nm peak associated with tryptophan.

X-Ray Structure Determination

N132A was crystallized by hanging drop vapor diffusion, equilibrating a 8-μL droplet containing 5 mg/ml N132A and 0.65 M sodium potassium phosphate (NaKPi) buffer, at pH 8.0, against a reservoir solution of 0.75 ml 1.4 M NaKPi buffer, at pH 8.0. Droplets were initially seeded with microcrystals of the TEM mutant M182T (X. Wang, G. Minasov, and B.K. Shoichet, unpublished results). N132A crystals were soaked with 7.5 mg/ml imipenem in 1.4 M NaKPi buffer, at pH 8.0, for 15 min and cryoprotected in 7.5 mg/ml imipenem, 25% sucrose in 1.6 M NaKPi buffer, at pH 8.0.

A crystal was mounted in a nylon loop and was flash-frozen in a nitrogen stream (100 K). X-ray diffraction data were collected on the 5-ID beamline (λ = 1.0000 Å) of the DND-CAT at the Advanced Photon Source (Argonne, IL), using a MARCCD detector. The data were processed and merged in the DENZO/SCALEPACK suite.[21] The M182T structure (X. Wang, G. Minasov, and B.K. Shoichet, unpublished results) was used as an initial model. After rigid group refinement and torsion angle annealing in CNS,[22] residue Ala132 and Met182 were fit into the |Fo − Fc| difference density map. Positive continuous density from Oγ of Ser70 in the active site indicated the presence of covalently bound imipenem. The initial imipenem model was built with angles and bond lengths according to the Cambridge Crystallographic Database.[23] The model was refined by cycles of Cartesian and *B*-factor refinement,[24] followed by manual correction with the Turbo program.[25] The simulated annealing |Fo − Fc| omit map indicated that imipenem was well ordered in the active site (see Fig. 5).

RESULTS

Two-State Reversible Thermal Denaturation of TEM-1

To analyze noncovalent interaction energies in the acyl adduct, it was necessary to show that TEM-1 could be denatured reversibly in a two-state manner. The enzyme was thermally denatured in 200 mM potassium phosphate buffer, pH 7.0, and monitored by far-UV CD (Fig. 3A). An average T_m value of 51.6°C and an average van't Hoff enthalpy (ΔH_{VH}) value of 139.5 kcal/mol were obtained at a ramp rate of 2°C/min (Table I). On rapid cooling, more than 95% of the original CD signal returned. When the unfolded enzyme was slowly cooled at 2°C/min back through the folding transition, an average T_m of 50.3°C and an average ΔH_{VH} of 100.2 kcal/mol were obtained. These results suggest that TEM-1 may be reversibly denatured by temperature.

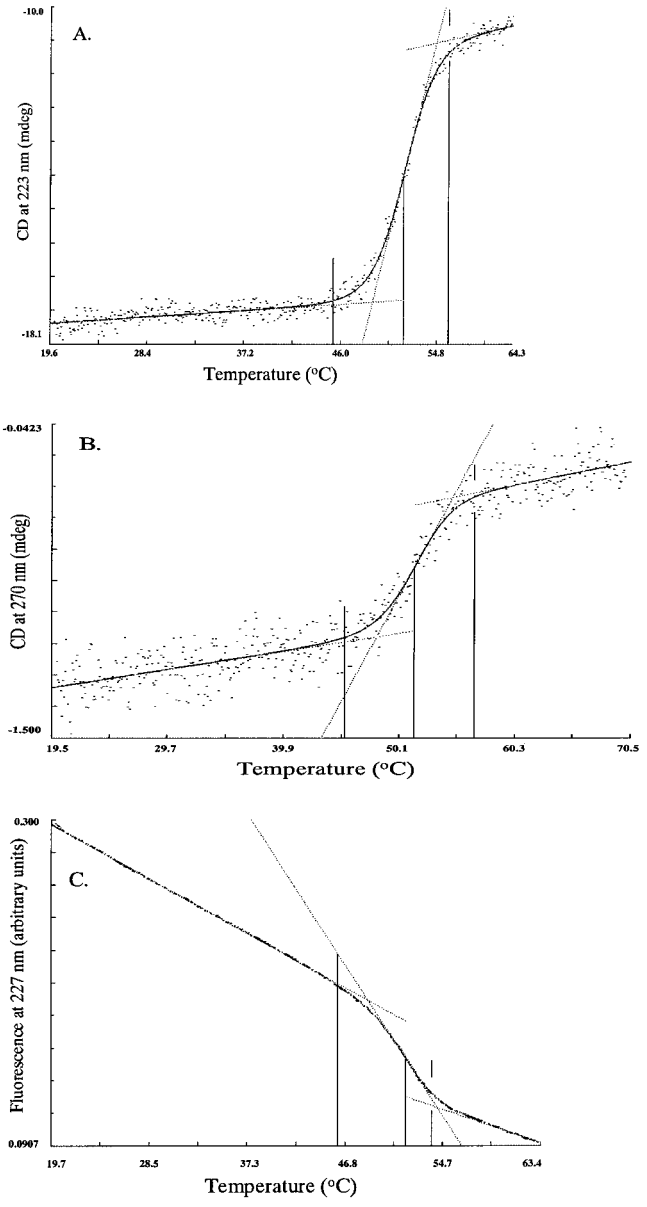

Fig. 3. Thermal denaturation of apo-TEM-1. Dotted lines, asymptotes of the upper and lower baselines and tangent to the transition region; solid line, least-squares fit to the data; vertical lines, melting region and the T_m. Values are given in Table I. **A:** Melting followed by far-ultraviolet (UV) circular dichroism (CD). **B:** Melting followed by near-UV CD. **C:** Melting followed by fluorescence.

TABLE I. Two-State Thermal Denaturation of TEM-1 and N132A

	Technique	T_m (°C)	ΔH_{VH} (kcal/mol)	ΔS_u (kcal/mol · K)
TEM-1	Far-UV CD	51.5 ± 0.2	139.5 ± 7.9	0.43 ± 0.02
	Near-UV CD	51.4 ± 0.2	109.0 ± 29.0	0.34 ± 0.09
	Fluorescence	51.6 ± 0.1	146.2 ± 3.3	0.45 ± 0.01
N132A	Far-UV CD	49.6 ± 0.1	136.0 ± 9.0	0.42 ± 0.03
	Fluorescence	49.6 ± 0.1	140.2 ± 9.7	0.43 ± 0.03

UV, ultraviolet; CD, circular dichroism; T_m, melting temperature; ΔH_{VH}, van't Hoff enthalpy of unfolding; ΔS_u, entropy of unfolding.

To determine whether thermal denaturation of TEM-1 occurs in a two-state manner, unfolding was monitored by three techniques. Denaturation of secondary structure was monitored by far-UV CD at 223 nm (Fig. 3A). Denaturation of tertiary structure was monitored by near-UV CD at 270 nm (Fig. 3B) and by fluorescence at 340 nm (Fig. 3C). For most melts, fluorescence and far-UV CD were determined simultaneously, in the same cuvette. The T_m and ΔH_{VH} values measured by all three techniques resembled each other closely (Table I), consistent with two-state thermal denaturation of TEM-1. Also, the average T_m and the average ΔH_{VH} of melting were independent of the ramp rate at 1, 1.5, and 2°C/min. These results are consistent with TEM-1 denaturing in a two-state manner.

Thermal Denaturation of TEM-1 With Inhibitors

Noncovalent interaction energies between TEM-1 and various ligands were determined by measuring the differential stability of the apo-enzyme versus the inhibitor adducts (Fig. 2); representative denaturation curves are shown in Figure 4. Three different types of ligands were used: β-lactamase-resistant β-lactams, such as imipenem; β-lactamase inhibitors, such as clavulanic acid; and two transition-state analogues (Table II).

Two α-substituted "β-lactamase-resistant" β-lactams, moxalactam and imipenem, were tested for their noncovalent interaction energies with TEM-1 in the acyl adduct. Both moxalactam and imipenem, which possess bulky 6(7)-α-substituents thought to be important for resistance to hydrolysis, destabilized TEM-1 by as much as 3.5°C or 1.6 kcal/mol (Table II).

Two clinically used β-lactamase inhibitors, clavulanic acid and tazobactam, were examined for their effect on TEM-1 stability. Both clavulanic acid and tazobactam destabilized the enzyme significantly (Table II). Whether this destabilization is caused by interactions with the ligands in their original acyl adducts or with the ligands after chemical rearrangements they are known to undergo over time from within the acyl adducts remains unclear.

To determine the effect of a transition-state analogue on the stability of TEM-1, the effects of compound 1 (*p*-nitrophenyl[[*N*-(phenylactetyl)amino]methyl]phosphonate) and compound 2 (a boronic acid analogue of nafcillin) were investigated. Compound 1 and its analogues have been studied extensively as β-lactamase inhibitors.[8,26] A significant stabilization was observed in the compound 1-TEM-1 complex, which had a 2.8°C increase in T_m (Table II and Fig. 4). Compound 2 is a reversible transition-state analogue[27] that stabilized TEM-1 by 3.7°C (Table II).

Thermal Denaturation of N132A With Inhibitors

In the X-ray crystal structure of TEM-1 in complex with imipenem, the side-chain of the conserved Asn132 appears to clash with the 6α-substituent of the inhibitor.[7,8,10] The α-face configuration (*R*-stereochemistry) of this side-chain is unusual—in most β-lactams, the R1 side-chains are on the β-face of the β-lactam ring, with a hydrogen atom on the α-face (*S*-stereochemistry). Replacing a hydrogen atom with a bulky side-chain is thought to be responsible for the inhibitory actions of β-lactams, such as imipenem, that contain 6α side-chains. This unusual stereochemistry also appears to cause the destabilization observed with these inhibitors. To test this hypothesis, N132A was made by site-directed mutagenesis and thermally denatured (Table I). N132A is 2.0°C (0.9 kcal/mol) less stable than wild-type, with a T_m value of 49.6°C. The mutant enzyme appears to denature in a reversible, two-state manner, as suggested by the more than 95% return of CD and fluorescence signals upon cooling, a T_m value of 49.5°C on re-melting of enzyme that had been through a previous round of denaturation and renaturation, and the correspondence of CD and fluorescence melting parameters (Table I).

The effects of several inhibitors were tested on N132A. In general, it took a higher concentration of inhibitor and longer pre-incubation time to achieve the same level of inhibition for N132A as for the wild-type enzyme, which was expected, given the lower activity of N132A (data not shown).[28] For each inhibitor, penicillinase activity of the acyl adduct of N132A was examined both before and after thermal denaturation, to ensure that the enzyme was completely inhibited, indicating the stable formation of the acyl adduct (data not shown). In contrast to wild-type, N132A is stabilized by moxalactam and imipenem by 1.2°C and 3.5°C, respectively (Table II). This responds a differential interaction energy change of 2.1 and 2.6 kcal/mol, respectively.

As a technical matter, we note that several of the inhibitors had considerable effects on the ΔH_{VH} of unfolding. This complicates comparison of ΔG_u values using equation 1,[19] which is easiest to justify when ΔH_{VH} values are similar. To minimize the effects of extrapolation and different ΔH_{VH} values, we also compared the unfolding equilibria directly at a reference temperature that lay in the middle of the range of observed T_m values. This was done using equation 2, which allowed us to use the ΔH_{VH} value that was measured for each curve. Using either equation had little quantitative effect (Table II) and had no qualitative effect on the results observed. The one exception might be the case of the imipenem covalent adduct with N132A, for which the ΔH_{VH} values differ considerably between the apo- and imipenem-bound enzymes. Imipenem acylation of N132A leads to an increased T_m by 3.5°C, but to a decreased ΔH_{VH} value relative to

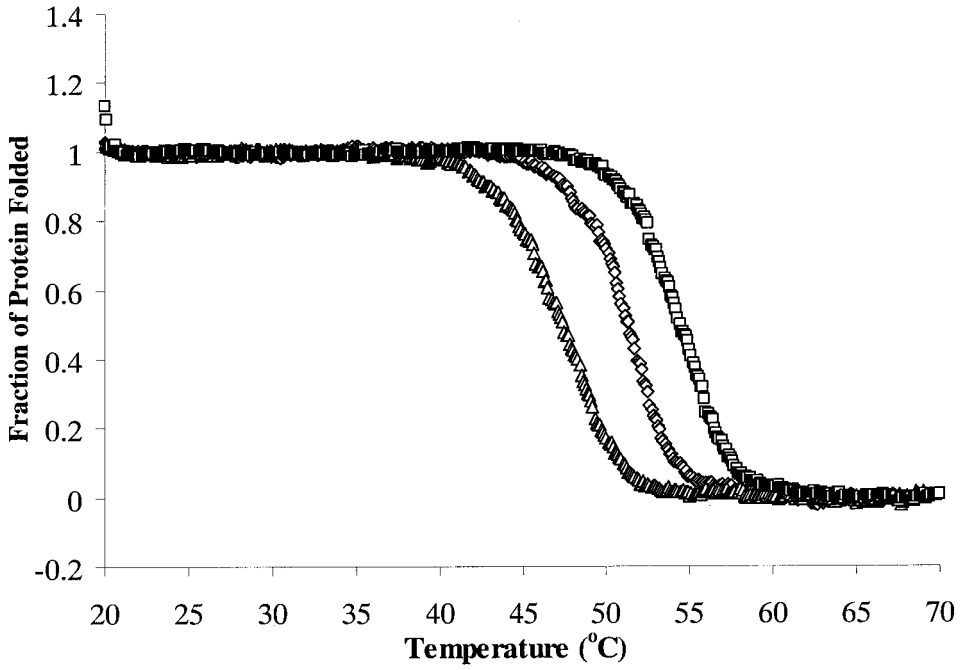

Fig. 4. Thermal denaturation of TEM-1 wild-type alone (diamonds), with imipenem (triangles), and with compound 1 (squares), as monitored by fluorescence. Values are given in Table II.

apo-enzyme. The stabilization of N132A by imipenem is reliable at the T_m, but the extrapolation to room temperature is less robust.

X-Ray Crystallographic Structure of N132A With Imipenem

To understand the stabilizing effect of imipenem on N132A as compared with its destabilizing effect on wild-type, the X-ray crystallographic structure of N132A complexed with imipenem was determined to 1.73 Å (Table III). The electron density for imipenem was well defined in the structure (Fig. 5). When analyzed by Procheck,[29] all residues except one were within the most favored areas of the Ramachandron plot, with residue 220 in an additionally allowed region. The final R-factor and R_{free} values of the refined structure were 16.1% and 19.3%, respectively. The atomic coordinates were deposited in Protein Data Bank (PDB) (code 1JVJ).

Compared with the WT complex,[7] imipenem adopts a very different conformation in the N132A complex [Fig. 6(A,B)]. In the complex with the WT enzyme, imipenem adopts a conformation where the former lactam oxygen has rotated by almost 180° relative to the conformation seen in every other β-lactam complex, such that it no longer sits in the "oxyanion"[30] or "electrophilic"[31] hole. This rotation may reflect the high-energy contact with Asn132 that would result from imipenem adopting a canonical conformation in the binding site. In contrast, in the N132A/imipenem complex, the lactam oxygen has flipped back into the "oxyanion" or "electrophilic" hole, forming hydrogen bonds with the backbone nitrogens of Ser70 and Ala237. The 6-α-hydroxyethyl group of the inhibitor occupies the cavity left by the Asn132 → Ala substitution (Fig. 7). In this conformation, the structure of the imipenem complex resembles that of other β-lactams in complex with β-lactam binding enzymes, such as the penicillin G/TEM-1 E166N complex[3] (Fig. 8). The rotation of the imipenem carbonyl allows Ser130 to flip back into a more usual conformation, reforming a hydrogen bond network with Lys73 and Lys234 that exists in most TEM structures but had been lost in the WT/imipenem complex as a result of the insertion of the lactam oxygen of the inhibitor. Tyr105, which had also changed conformation in the WT complex, also relaxes back into a more canonical conformation. In addition to the internal hydrogen bonds between enzyme side-chains that are re-formed, imipenem makes seven hydrogen bonds with the enzyme in the N132A complex, compared with three hydrogen bonds observed in the WT complex.[7] Despite the significant inhibitor and side-chain conformational changes, the overall structure of N132A/imipenem resembles that of other TEM-1 complexes, differing from the penicillin G/TEM-1 complex by 0.27 Å root-mean-square deviation (RMSD) in Cα positions, and differing from the WT/imipenem by 0.33 Å RMSD in Cα positions.

DISCUSSION

Paradoxically, all the β-lactams reported in this study have unfavorable noncovalent interaction energies in their acyl adducts with TEM-1. The primary driving force for β-lactam binding is the formation of the covalent adduct. Once formed, the noncovalent interaction energies within this adduct can be favorable or unfavorable, in the same way that a substituted residue can either stabilize or destabilize a protein. Thus, ligand complementarity in covalent adducts can be very different from reversible

TABLE II. Differential Thermal Stability of β-Lactam Adducts With TEM-1 and N132A

		TEM-1 wild-type[a] (T_m = 51.6°C; ΔH_{VH} = 146.2 kcal/mol)			TEM N132A (T_m = 49.6°C; ΔH_{VH} = 140.2 kcal/mol)		
Ligand	Ligand structure	ΔT_m (°C)	ΔH_{VH} (kcal/mol)	$\Delta\Delta G_u$ (kcal/mol)	ΔT_m (°C)	ΔH_{VH} (kcal/mol)	$\Delta\Delta G_u$ (kcal/mol)
Moxalactam	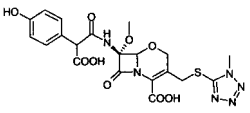	−3.5 ± 0.2	74.1 ± 7.7	−1.6 ± 0.1[b] (−0.97)[c]	1.2 ± 0.1	101.5 ± 5.3	0.53 ± 0.07 (0.35)
Imipenem	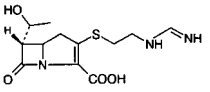	−2.7 ± 0.1	147.4 ± 12.9	−1.1 ± 0.1 (−1.3)	3.5 ± 0.1	102.8 ± 5.2	1.5 ± 0.1 (1.1)
Clavulanic acid	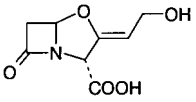	−5.5 ± 0.2	71.7 ± 4.1	−2.5 ± 0.1 (−1.5)	−1.1 ± 0.2	73.1 ± 3.8	−0.48 ± 0.09 (−0.28)
Tazobactam	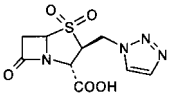	−2.6 ± 0.1	84.1 ± 0.5	−1.2 ± 0.1 (−0.75)	ND[d]	ND	ND
Compound 1	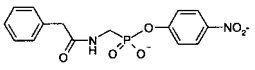	2.8 ± 0.2	129.6 ± 7.0	1.3 ± 0.1 (1.0)	ND	ND	ND
Compound 2	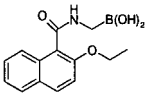	3.7 ± 0.1	185.1 ± 15.4	1.7 ± 0.1 (2.5)	0.4 ± 0.1	151.4 ± 12.3	0.17 ± 0.04 (0.17)

[a]Determined using fluorescence spectra.
[b]Determined by Schellman's method[19]: $\Delta\Delta G_u = \Delta T_m \cdot \Delta S_{apo\text{-}enzyme}$. $\Delta S_{apo\text{-}enzyme}$ for wild-type is 0.45 ± 0.01 kcal/mol · K, and $\Delta S_{apo\text{-}enzyme}$ for N132A is 0.44 ± 0.03 kcal/mol · K.
[c]Average $\Delta\Delta G_u$ by using eq 2; see Materials and Methods.
[d]Not determined.

TABLE III. Crystallographic Data Collection and Refinement Statistics for the N132A/Imipenem Structure*

Unit cell parameters (Å)	a = 41.30; b = 61.69; c = 89.14
Resolution (Å)	1.73 (1.79–1.73)[a]
Unique reflections	23324
Total observations	125788
R_{merge} (%)	5.0 (25.0)
Completeness (%)	95.3 (98.0)
$\langle I \rangle \langle \sigma_I \rangle$	26.5 (6.1)
Resolution range for refinement (Å)	15.0–1.73
No. of protein residues	263
No. of potassium ions	5
No. of water molecules	418
RMSD bond lengths (Å)	0.009
RMSD bond angles (°)	1.53
R-factor (%)	16.1
R_{free} (%)	19.3[a]
Average B-factor, protein atoms (Å^2)	12.8
Average B-factor, inhibitor atoms (Å^2)	19.1
Average B-factor, solvent atoms (Å^2)	26.4

*Values in parentheses are for the highest resolution shell.
[a]R_{free} was calculated with 10% of reflections set aside randomly.

inhibitors, such as compound 2, which must stabilize the enzyme, assuming they bind preferentially to its folded form.

Perhaps the most interesting cases to consider are those of imipenem and moxalactam. Based on the crystal structure of the imipenem/WT complex,[7] the unfavorable interaction between the enzyme and these inhibitors appears to owe to the presence of an unusual 6(7)-α-substituent that both imipenem and moxalactam contain[10] (see also the discussion of a related effect in the class C β-lactamase AmpC[10,15,16]). This group appears to force the side-chain of Asn132 to move, displacing the amide nitrogen by 1.7 Å and the amide oxygen by 1.0 Å.[7] More dramatically, the close contact with Asn132 appears to cause the imipenem carbonyl oxygen to flip by nearly 180°, so that it no longer sits in the "oxyanion" or "electrophilic" hole of TEM-1,[7] as would be expected for a β-lactam acyl adduct.

To test the hypothesis that Asn132 is in steric conflict with moxalactam and imipenem, we substituted Asn132 with Ala and measured the stability of the mutant enzyme with imipenem and moxalactam. Compared with the complex with TEM-1 wild-type, we observed a stabilizing $\Delta\Delta T_m$ of 6.2°C (where $\Delta\Delta T_m$ is the difference between ΔT_m

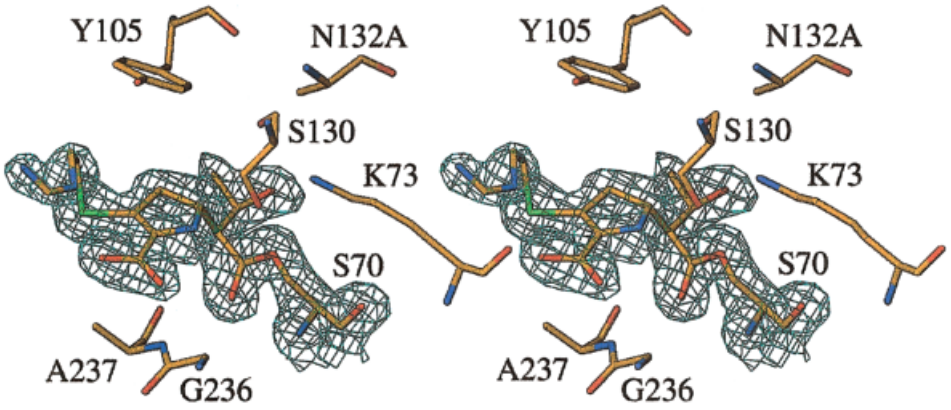

Fig. 5. Stereoview of simulated annealing |Fo − Fc| omit electron density (cyan) of N132A in complex with imipenem, contoured at 3σ. Selected residues and imipenem are shown. Carbon, oxygen, nitrogen, and sulfur atoms are colored yellow, red, blue, and green, respectively.

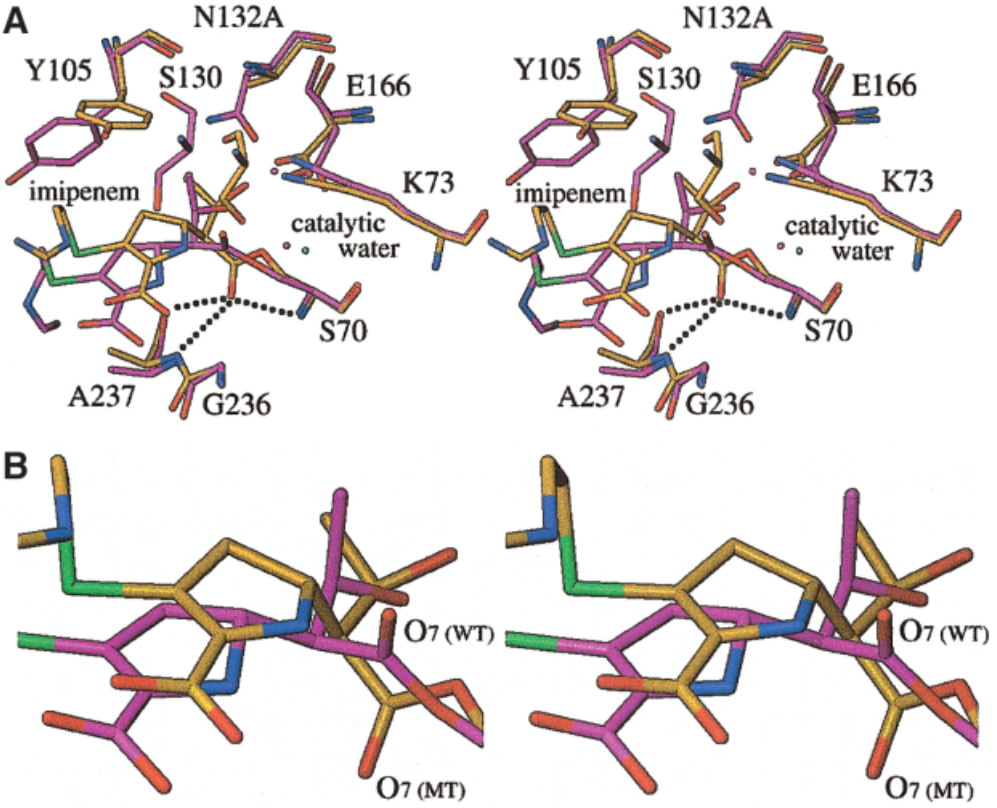

Fig. 6. Stereoview of superposition of the wild-type (WT)/imipenem (carbons in magenta) and the N132A/imipenem complexes (carbons in yellow). Other atoms are colored as in Fig. 5, except for the N132A water (cyan) and the WT water (magenta). Dashed lines represent interactions between the imipenem carbonyl oxygen and the enzyme atoms making up the "electrophilic" hole (see Table IV for distances). **A:** Overview of the active site. **B:** Enlarged view around the imipenem–Ser70 acyl– complex showing the different conformation of the ester carbonyl oxygen.

from apo- to imipenem-bound wild-type and ΔT_m from apo- to imipenem-bound N132A) and a $\Delta\Delta G_u$ of 2.6 kcal/mol for the N132A/imipenem complex (Table II). Unlike the wild-type complex, moxalactam and imipenem actually stabilize the mutant enzyme to thermal denaturation. In the X-ray crystallographic structure of the imipenem/N132A complex, the 6-α-hydroxyethyl of imipenem fills the cavity created by the Asn132 → Ala substitution (Fig. 7), allowing the ester carbonyl oxygen to flip back into "electrophilic" hole. This restores the former lactam carbonyl oxygen to a canonical conformational, resembling that adopted by penicillin G in a complex with a TEM-1 mutant[3] (Fig. 8). In turn, this restores two hydrogen bonds to the lactam oxygen that were lost in the imipenem/WT

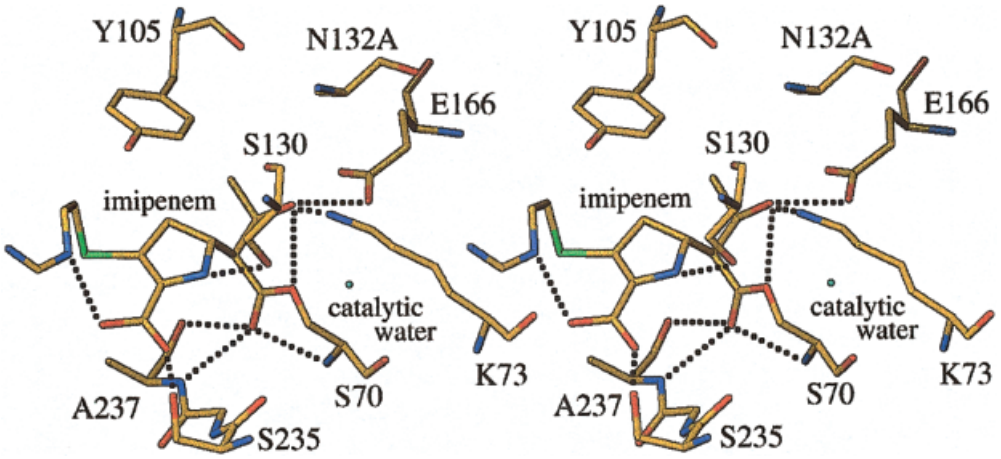

Fig. 7. Stereoview of the active site of N132A in the complex with imipenem. All atoms are as Fig. 5, except the catalytic water, which is colored in cyan. Dashed lines represent hydrogen bonds and one polar interaction (between the carbonyl oxygen of Ala237 and the O7 of imipenem).

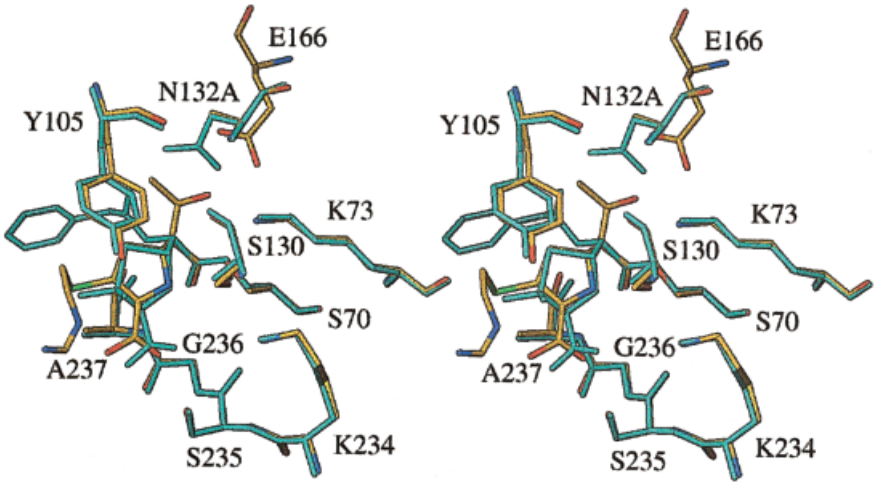

Fig. 8. Stereoview of a superposition of the N132A/imipenem (colored as in Fig. 5) and the TEM E166N/penicillin G (cyan) complexes.

complex [Fig. 6(A,B)]. Overall, imipenem makes seven hydrogen bonds to N132A and only three to the wild-type enzyme. Moreover, this conformational change allows Ser130 and Tyr105 to relax back into the conformations they typically adopt in TEM-1. This restores hydrogen bonds between Ser130, Lys73, and Lys234, and between Ser130 and the penem nitrogen of imipenem (Fig. 7 and Table IV). These results are consistent with a model where a steric clash between Asn132 and the 6(7)-α group of imipenem or moxalactam is largely responsible for the destabilizing effects of these inhibitors on TEM-1,[7] and for the unusual conformation that imipenem adopts in the imipenem/WT structure. The substitution Asn132 → Ala removes this unfavorable contact, allowing imipenem to flip back into a canonical conformation, stabilizing the acyl enzyme, rather than destabilizing it. We note that the complementarity of N132A comes at a cost to its own internal stability, which is reduced versus WT, presumably because of the creation of a packing defect and to the loss of a hydrogen bond with Lys73. The loss of the hydrogen bond made by Asn132 to the catalytically key Lys73 may also explain the very low activity of N132A, which is only 0.03% that of WT.[28,32]

The destabilizing interactions that imipenem and moxalactam have in their TEM-1 acyl adducts may offer insights into the evolution of resistance to these drugs and suggest an unusual design protocol for improved inhibitors. There are more than 90 clinically occurring TEM-1 mutants that have either an extended spectrum of action against β-lactams (ESBL) or that are inhibitor resistant (IRT) (http://www.lahey.org/studies/temtable.htm). To date, none has have significant activity against imipenem-like β-lactams,[33] which we hypothesize is because of the incompatibility of 6(7)-α-substituent with the completely conserved Asn132. Although N132A is compatible with the bulky 6(7)-α-substituents in moxalactam and imipenem, this mutant does not pose a threat to public health because of its very low activity. A more serious concern is that three

TABLE IV. Comparison Between Interactions Observed in the Imipenem Complex With N132A and the Imipenem Complex With Wild-Type TEM-1

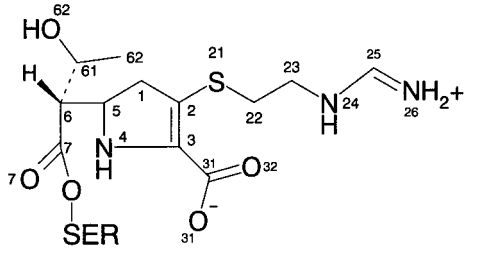

Interaction	Distance (Å) N132A/imipenem	Distance (Å) WT/imipenem[a]
Catalytic water–S70 Oγ	3.1	3.0
Catalytic water–E166 Oε2	2.8	2.5
Catalytic water–N170 Nδ	2.8	2.6
N132 Oδ–K73 Nζ	—	3.3
S70 Oγ–K73 Nζ	3.0	4.1
S130 Oγ–K73 Nζ	3.0	6.1
S130 Oγ–K234 Nζ	2.7	4.3
Imipenem O7–S70 N	2.7	4.7
Imipenem O7–A237 N	2.9	5.4
Imipenem O7–A237 O	3.2	5.8
Imipenem O7–S130 Oγ	4.7	3.3
Imipenem O62–N132 Oδ	—	2.7
Imipenem O62–K73 Nζ	2.8	4.0
Imipenem O62–E166 Oε2	2.6	3.2
Imipenem O62–S70 Oγ	3.0	3.6
Imipenem O62–catalytic water	3.4	2.6
Imipenem O31–S235 Oγ	2.8	3.1
Imipenem N4–S130 Oγ	2.8	3.9
Imipenem N4–imipenem O32	2.6	5.5

[a]From the crystallographic structure (PDB 1BT5) by Maveyraud et al.[7]

closely related class A β-lactamases, SME-1, IMI-1, and NMC-A, have significant imipenemase activity.[34–36] All three enzymes conserve Asn132.[36] Intriguingly, the X-ray crystallographic structure of apo-NMC-A shows that the side-chain of Asn132 is displaced by 1.0 Å from its position in other class A enzymes.[37] The movement of Asn132 in NMC-A may allow it to accommodate the bulky 6(7)-α-substituent without the rearrangements seen in the imipenem/TEM-1 complex, and without distorting the interaction between Asn132 with Lys73.[37] The structural similarity among NMC-A, TEM-1, and other class A β-lactamases raises concern that secondary mutations in widespread β-lactamases, such as TEM-1, might emerge that displace Asn132, allowing these enzymes to hydrolyze imipenem and moxalactam. One paradoxical implication of this study might be that to combat such mutant β-lactamases, one should design even bulkier 6(7)-α-substituents, which will disrupt the mutant enzymes in the same way that the current substituents disrupt TEM-1. Such a structure-based design program would focus on the creation not of complementary interactions, as is commonly done, but of anti-complementary interactions that will disrupt the ability of the acyl adduct, once formed, to adopt a catalytically competent conformation.

ACKNOWLEDGMENTS

The authors thank Rex Pratt for the gift of the phosphonate inhibitor compound 1, Emilia Caselli and Fabio Prati for compound 2, Robert Bonomo for clavulanic acid, Eli Lilly for tazobactam, Jesús Blazquez for imipenem, Doug Barrick for suggesting the direct comparison of unfolding equilibria, Beth Beadle for technical advice, and Robert G. Kemp for pZR3. We thank Beth Beadle, John Irwin, Indi Trehan, Susan McGovern, and Alexandra Patera for reading this manuscript. X-ray crystallographic data were collected at the DuPont–Northwestern–Dow Collaborative Access Team (DND–CAT) synchrotron Research Center at the Advanced Photon Source (APS). DND–CAT is supported by the DuPont Co., Dow Chemical Co., National Science Foundation, and the State of Illinois. Use of the APS is supported by the U.S. Department of Energy under contract W-31-102-Eng-38.

REFERENCES

1. Livermore DM. β-Lactamases in laboratory and clinical resistance. Clin Microbiol Rev 1995;8:557–584.
2. Lejeune A, Vanhove M, Lamotte-Brasseur J, Frere JM, Matagne A. Quantitive analysis of the stabilization by substrate of *Staphylococcus aureus* PC1 β-lactamase. Chem Biol 2001;8:831–842.
3. Strynadka NC, Adachi H, Jensen SE, Johns K, Sielecki A, Betzel C, Sutoh K, James MN. Molecular structure of the acyl-enzyme intermediate in β-lactam hydrolysis at 1.7 Å resolution. Nature 1992;359:700–705.
4. Chen CC, Herzberg O. Inhibition of β-lactamase by clavulanate. Trapped intermediates in cryocrystallographic studies [published erratum appears in J Mol Biol 1992;226:285]. J Mol Biol 1992;224:1103–1113.
5. Chen CC, Rahil J, Pratt RF, Herzberg O. Structure of a phosphonate-inhibited β-lactamase. An analog of the tetrahedral transition state/intermediate of β-lactam hydrolysis. J Mol Biol 1993;234:165–178.
6. Jelsch C, Mourey L, Masson JM, Samama JP. Crystal structure of *Escherichia coli* TEM-1 β-lactamase at 1.8 Å resolution. Proteins 1993;16:364–383.
7. Maveyraud L, Mourey L, Kotra LP, Pedelacq JD, Guillet V, Mobashery S, Samama JP. Structural basis for clinical longevity of carbapenem antibiotics in the face of challenge by the common class A β-lactamases from the antibiotic-resistant bacteria. J Am Chem Soc 1998;120:9748–9752.
8. Rahil J, Pratt RF. Characterization of covalently bound enzyme inhibitors as transition-state analogs by protein stability measurements: phosphonate monoester inhibitors of a β-lactamase. Biochemistry 1994;33:116–125.
9. Morton A, Baase WA, Matthews BW. Energetic origins of specificity of ligand binding in an interior nonpolar cavity of T4 lysozyme. Biochemistry 1995;34:8564–8575.
10. Beadle BM, McGovern SL, Patera A, Shoichet BK. Functional analyses of AmpC β-lactamase through differential stability. Protein Sci 1999;8:1816–1824.
11. Beadle BM, Nicholas RA, Shoichet BK. Interaction energies between β-lactam antibiotics and *E. coli* penicillin-binding protein 5 by reversible thermal denaturation. Protein Sci 2001;10:1254–1259.
12. Bush K. β-Lactamases of increasing clinical importance. Curr Pharm Des 1999;5:839–845.
13. Knox JR, Moews PC, Frere JM. Molecular evolution of bacterial β-lactam resistance. Chem Biol 1996;3:937–947.
14. Massova I, Mobashery S. Kinship and diversification of bacterial penicillin-binding proteins and β-lactamases. Antimicrob Agents Chemother 1998;42:1–17.
15. Patera A, Blaszczak LC, Shoichet BK. Crystal structures of substrate and inhibitor complexes with AmpC-lactamase: possible implications for substrate-assisted catalysis. J Am Chem Soc 2000;122:10504–10512.
16. Trehan I, Beadle BM, Shoichet BK. Inhibition of AmpC beta-

lactamase through a destabilizing interaction in the active site. Biochemistry 2001;40:7992–7999.
17. Dubus A, Wilkin JM, Raquet X, Normark S, Frere JM. Catalytic mechanism of active-site serine beta-lactamases: role of the conserved hydroxy group of the Lys-Thr(Ser)-Gly triad. Biochem J 1994;301(pt 2):485–494.
18. Ho SN, Hunt HD, Horton RM, Pullen JK, Pease LR. Site-directed mutagenesis by overlap extension using the polymerase chain reaction. Gene 1989;77:51–59.
19. Becktel WJ, Schellman JA. Protein stability curves. Biopolymers 1987;26:1859–1877.
20. Kirchhoff W. EXAM: a two-state thermodynamic analysis program. Gaithersburg, MD; 1993.
21. Otwinowski Z, Minor W. Processing of X-ray diffraction data collected in oscillation mode. Methods Enzymol 1997;276:307–326.
22. Brünger AT, Adams PD, Clore GM, DeLano WL, Gros P, Grosse-Kunstleve RW, Jiang JS, Kuszewski J, Nilges M, Pannu NS, Read RJ, Rice LM, Simonson T, Warren GL. Crystallography and NMR system: a new software suite for macromolecular structure determination. Acta Crystallogr D Biol Crystallogr 1998;54(pt 5):905–921.
23. Bruno IJ, Cole JC, Lommerse JP, Rowland RS, Taylor R, Verdonk ML. IsoStar: a library of information about nonbonded interactions. J Comput Aided Mol Des 1997;11:525–537.
24. Engh RA, Huber R. Accurate bond and angle parameters for X-ray protein structure refinement. Acta Crystallogr 1991;A47:392–400.
25. Cambillau C, Roussel A. Turbo Frodo. Université Aix-Marseille II, Marseille, France; 1997.
26. Li N, Rahil J, Wright ME, Pratt RF. Structure–activity studies of the inhibition of serine β-lactamases by phosphonate monoesters. Bioorg Med Chem 1997;5:1783–1788.
27. Caselli E, Powers RA, Blasczcak LC, Wu CY, Prati F, Shoichet BK. Energetic, structural, and antimicrobial analyses of β-lactam side chain recognition by β-lactamases. Chem Biol 2001;8:17–31.
28. Jacob F, Joris B, Lepage S, Dusart J, Frere JM. Role of the conserved amino acids of the 'SDN' loop (Ser130, Asp131 and Asn132) in a class A β-lactamase studied by site-directed mutagenesis. Biochem J 1990;271:399–406.
29. Laskowski RA, MacArthur MW, Moss DS, Thornton JM. PROCHECK: a program to check the stereochemical quality of protein structures. J Appl Crystallogr 1993;26:283–291.
30. Murphy BP, Pratt RF. Evidence for an oxyanion hole in serine beta-lactamases and DD-peptidases. Biochem J 1988;256:669–672.
31. Usher KC, Blaszczak LC, Weston GS, Shoichet BK, Remington SJ. Three-dimensional structure of AmpC β-lactamase from *Escherichia coli* bound to a transition-state analogue: possible implications for the oxyanion hypothesis and for inhibitor design. Biochemistry 1998;37:16082–16092.
32. Osuna J, Viadiu H, Fink AL, Soberon X. Substitution of Asp for Asn at position 132 in the active site of TEM β-lactamase. Activity toward different substrates and effects of neighboring residues. J Biol Chem 1995;270:775–780.
33. Livermore DM. β-Lactamase-mediated resistance and opportunities for its control. J Antimicrob Chemother 1998;41 suppl D:25–41.
34. Naas T, Nordmann P. Analysis of a carbapenem-hydrolyzing class A β-lactamase from *Enterobacter cloacae* and of its LysR-type regulatory protein. Proc Natl Acad Sci USA 1994;91:7693–7697.
35. Rasmussen BA, Bush K, Keeney D, Yang Y, Hare R, O'Gara C, Medeiros AA. Characterization of IMI-1 β-lactamase, a class A carbapenem-hydrolyzing enzyme from *Enterobacter cloacae.* Antimicrob Agents Chemother 1996;40:2080–2086.
36. Nordmann P, Mariotte S, Naas T, Labia R, Nicolas MH. Biochemical properties of a carbapenem-hydrolyzing β-lactamase from *Enterobacter cloacae* and cloning of the gene into *Escherichia coli.* Antimicrob Agents Chemother 1993;37:939–946.
37. Swaren P, Maveyraud L, Raquet X, Cabantous S, Duez C, Pedelacq JD, Mariotte-Boyer S, Mourey L, Labia R, Nicolas-Chanoine MH, Nordmann P, Frere JM, Samama JP. X-ray analysis of the NMC-A β-lactamase at 1.64-Å resolution, a class A carbapenemase with broad substrate specificity. J Biol Chem 1998;273:26714–26721.